Interplay of the charged Higgs boson effects in $R_{D^{(*)}}$, $b \to s\ell^+\ell^-$, and W mass

Girish Kumar
Department of Physics, National Taiwan University, Taipei 10617, Taiwan

(Received 2 January 2023; accepted 29 March 2023; published 17 April 2023)

Current data on semileptonic charged- and neutral-current B decays show deviations from the predictions of the Standard Model. It is well known that a charged Higgs boson, belonging to the two-Higgs doublet model without Z_2 symmetry, offers one of the simplest solution to the charged-current B decays. We show that this solution naturally induces a negative shift of $\mathcal{O}(1)$ in the Wilson coefficient ($C_{9\ell}$) of operator $(\bar{s}_L\gamma_\mu b_L)(\bar{\ell}\gamma^\mu\ell)$, potentially resolving the tension in neutral-current B decays as well. Interestingly, the lepton universality ratios in $b \to s\ell^+\ell^-$ decays, in tune with the recent LHCb result, remain SM-like. Precision constraints from neutral B and K meson mixing, decays $B_c \to \tau\bar{\nu}$, $B \to X_s\gamma$, and leptonic decays of τ and Z can be satisfied. Furthermore, a positive shift in W-boson mass, nicely in agreement with the CDF measurement, is also possible, requiring the neutral scalars to be heavier than the charged Higgs but within the sub-TeV region.

DOI: 10.1103/PhysRevD.107.075016

I. INTRODUCTION

It is remarkable that though there already exists irrefutable experimental evidence (e.g., baryon asymmetry of the Universe, neutrino masses) and persuasive theoretical reasons (e.g., naturalness problem, flavor problem) for physics beyond the Standard Model (SM), no new physics (NP) particle has turned up so far at the LHC. One reason could be that the NP scale is very heavy and beyond LHC reach. However, in recent years a number of measurements, especially those associated with semileptonic decays of B mesons, have been significantly at odds with the SM predictions and could be telltale sign of sub-TeV scale NP accessible at the LHC. We discuss one example of such NP—a charged Higgs boson (H^+) of a few hundred GeV mass, which can help in alleviating the tension between theory and the current data.

In semileptonic B decays, one set of prominent anomalies, persisting for many years and strengthened further by the recent LHCb measurement [1], are in the lepton flavor universality (LFU) ratios

$$R_{D^{(*)}} = \frac{\mathrm{BR}(B \to D^{(*)}\tau\bar{\nu})}{\mathrm{BR}(B \to D^{(*)}\ell\bar{\nu})}; \qquad \ell = \{e, \mu\}. \qquad (1)$$

The current world average by HFLAV [2], based on measurements by B factories [3–7] and LHCb [1,8–10], gives $R_D = 0.358 \pm 0.028$ and $R_{D^*} = 0.285 \pm 0.013$. Individually, these values disagree with the SM expectation [11–18] at the significance level of 2.2σ and 2.3σ, respectively. Taken together (the correlation coefficient is -0.29), the disagreement increases to 3.2σ.[1] On the other hand, measurements of analogous muon vs electron LFU ratios are in agreement with the SM predictions [22–24].

Another set of anomalies are observed in $b \to s\mu^+\mu^-$ decays. One of these is the $\sim 3\sigma$ anomaly in the measurement of angular observable P_5' in the decay $B \to K^*\mu^+\mu^-$ [25–27]. Another sizable tension, of 3.6σ significance, is reported by LHCb [28–30] in the measurement of branching fraction of the $B_s \to \phi\mu^+\mu^-$ decay, finding it below the SM expectation. The data on $B \to K\mu^+\mu^-$ [31] and $\Lambda_b \to \Lambda\mu^+\mu^-$ [32] also show a deficit in branching fractions with respect to the SM predictions. The recent update from LHCb [33,34] however finds no evidence of LFU breaking in $b \to s\ell^+\ell^-$ decays: the ratios $R_{K^{(*)}} = \mathrm{BR}(B \to K^{(*)}\mu^+\mu^-)/\mathrm{BR}(B \to K^{(*)}e^+e^-)$ [35] measured in the dilepton invariant mass bins $0.1 < q^2 < 1.1\ \mathrm{GeV}^2$ and $1.1 < q^2 < 6\ \mathrm{GeV}^2$

[1]The trend of surplus in tauonic modes is also observed in the measurement of $R_{J/\psi}$ [19], the LFU ratio defined similar to Eq. (1) for $B_c \to J/\psi$ transition, while the ratio R_{Λ_c} (related to $\Lambda_b \to \Lambda_c$ transition) shows a relative deficit [20]. These deviations, however, are relatively mild in significance as the current associated experimental uncertainties are large. We therefore do not include these two ratios in our analysis. We refer to a recent paper [21] analyzing the impact of R_{Λ_c} inclusion in NP analysis.

are in complete agreement[2] with the SM predictions known with percent-level accuracy [36–38]. These new findings overturn previous results [39–41] that reported a deficit in $R_{K^{(*)}}$. Although the predictions of individual branching fractions and optimized angular observables such as P_5' are subject to significant hadronic uncertainties [42–52]; at present it is contestable whether the long-distance effects can fully account for the tension in $b \to s\ell^+\ell^-$, and NP may be warranted to explain the data (e.g., see Ref. [53]).

Recently, the Fermilab CDF collaboration [54], based on 2002–2011 data with 8.8 fb^{-1} integrated luminosity, reported a new measurement of W-boson mass:

$$M_W = 80.4335 \pm 0.0094 \text{ GeV}, \tag{2}$$

which differs from the SM prediction $M_W^{\rm SM} = 80.357 \pm 0.006$ GeV [55] with 7σ significance. It is intriguing to note that the CDF measurement also differs with M_W measurements reported by ATLAS [56] and LHCb [57], an issue to be resolved[3] in the future with improved measurements. Here, we will take a view that the CDF measurement hints towards NP presence in the M_W value.

In this article we show that a H^+ boson, naturally present in simple extensions of the SM such as two-Higgs doublet model (2HDM) [59], can account for the above-mentioned anomalies. The fact that H^+ can explain R_D and R_{D^*} anomalies is well known in literature [60–77]. Here, we show that same set of H^+ interactions that explain the $R_{D^{(*)}}$ anomaly unavoidably induce a destructive NP contribution desired to simultaneously explain the tension in $b \to s\ell^+\ell^-$, while keeping the ratios $R_{K^{(*)}}$ unaltered. Our results strengthen the viewpoint that a common NP could be behind the charged- and neutral-current B anomalies. The M_W anomaly can also be explained by a NP contribution to the Peshkin-Takeuchi T parameter [78], which helps determine the allowed mass range of the physical scalars in the 2HDM.

II. H^+ INTERACTIONS AND RELEVANT NP PARAMETERS

The H^+ boson we consider belongs to a 2HDM without any special discrete symmetry (see Ref. [79] for a comprehensive review). The general H^+ interactions in the fermion mass basis are given by the Lagrangian [80]

$$\mathcal{L}_{H^+} = -\bar{u}(V\rho^d R - \rho^{u\dagger} V L) d H^+ - \bar{\nu}\rho^e \mathrm{Re} H^+ + \text{H.c.}, \tag{3}$$

where ρ^f ($f = u, d, e$) are 3×3 NP Yukawa matrices, V denotes the Cabibbo-Kobayashi-Maskawa (CKM) matrix, and $L/R \equiv (1 \mp \gamma_5)/2$ are the chirality projectors. In addition to the H^+ boson, 2HDM also has CP-even/odd scalar bosons H, A. Their Yukawa interactions are not important for our analysis; we refer to Refs. [80,81] for their details. However we need to define the masses of H, A, as those would be required in the computation of M_W in the model. The masses of H, A are related to mass of H^+ by the relations[4]

$$m_{H^+}^2 = m_H^2 - \frac{v^2}{2}(\Lambda_4 + \Lambda_5), \qquad m_A^2 = m_H^2 - v^2\Lambda_5, \tag{4}$$

where $v \simeq 246$ GeV, and Λ_4, Λ_5 are the quartic couplings in the Higgs potential (see the Appendix for details).

To explain the anomalies with a minimal set of NP parameters, we make the ansatz that NP Yukawa matrices have the following simple structure

$$\rho^u = \begin{pmatrix} 0 & 0 & 0 \\ 0 & 0 & 0 \\ 0 & \rho_{tc} & 0 \end{pmatrix}, \qquad \rho^e = \begin{pmatrix} 0 & 0 & 0 \\ 0 & 0 & 0 \\ 0 & 0 & \rho_{\tau\tau} \end{pmatrix}, \tag{5}$$

and $\rho^d = 0$. The texture, such as in Eq. (5), is the most economical choice to affect rate of $B \to D^{(*)}\tau\bar{\nu}$ only: the off-diagonal coupling ρ_{tc} facilitates H^+ mediated $b \to c$ transitions that are not CKM suppressed, and diagonal lepton coupling $\rho_{\tau\tau}$ ensures that only semitauonic modes are affected. With the above choice the Lagrangian in Eq. (3) simplifies to (dropping a V_{td} suppressed term)

$$\mathcal{L}_{H^+} = (\rho_{tc}^* V_{tb} \bar{c}_R b_L + \rho_{tc}^* V_{ts} \bar{c}_R s_L - \rho_{\tau\tau} \bar{\nu}_{\tau L} \tau_R) H^+ + \text{H.c.}, \tag{6}$$

which together with Eq. (4) defines all the Yukawa interactions and NP parameters relevant in our setup.

Concerning direct search constraints on H^+, analyses in Refs. [76,84], based on experimental results of Refs. [85–88], find that the mass range $m_{H^+} > 400$ GeV for an explanation of the $R_{D^{(*)}}$ anomaly is likely ruled out due to a constraint from the $pp \to bc \to \tau\nu$ process. However, the low-mass region $m_{H^+} < 400$ is still not excluded [76]. It was pointed out recently [77] that the $\tau\nu$ search with an additional b-tagged jet ($pp \to bH^\pm \to b\tau\nu$) could be useful in probing this low-mass region of H^+. In this article we therefore focus on the $m_{H^+} < 400$ GeV region.

[2]It is worth noting that rates of both the $B^+ \to K^+\mu^+\mu^-$ [31] and $B^+ \to K^+e^+e^-$ decays in the central q^2 bin are now low compared to the corresponding SM predictions while their ratio (R_K) remains SM-like [34].

[3]Recently it has been suggested [58] that discrepancies between different M_W measurements could be due to a light NP particle modifying the missing transverse momentum in the detector.

[4]Here we assume, in accordance with the current data [82,83], that there is very little mixing between the SM Higgs (h) and H boson.

III. OBSERVABLES

In this section we discuss H^+ contributions to the anomalous observables together with the relevant constraint on our setup.

A. R_D and R_{D^*}

The H^+ boson mediates $b \to c\tau\bar{\nu}$ transition at tree level [shown in Fig. 1(a)], the effect of which can be parametrized by the following effective Hamiltonian

$$\mathcal{H}_{\rm eff} = 2\sqrt{2}G_F V_{cb} C_{S,L} (\bar{c}_R b_L)(\bar{\tau}_R \nu_{\tau L}), \tag{7}$$

where the coefficient $C_{S,L}$ at scale $\mu \sim m_{H^+}$ is given by

$$C_{S,L} = \frac{\rho^*_{tc}\rho^*_{\tau\tau}}{2\sqrt{2}G_F V_{cb} m^2_{H^+}}. \tag{8}$$

The contributions of $C_{S,L}$ to ratios R_D and R_{D^*} are numerically parametrized (at scale $\mu \sim m_b$) as [89][5]

$$R_D \simeq (R_D)_{\rm SM}[1 + 1.49\,{\rm Re}(C_{S,L}) + 1.01|C_{S,L}|^2], \tag{9}$$

$$R_{D^*} \simeq (R_{D^*})_{\rm SM}[1 - 0.11\,{\rm Re}(C_{S,L}) + 0.04|C_{S,L}|^2]. \tag{10}$$

The scalar interaction in Eq. (7) contributes rather significantly (due to lack of chirality suppression) to the $B_c \to \tau\nu$ branching ratio. Numerically, it is given as [89]

$${\rm BR}(B_c \to \tau\nu) \simeq 0.02|1 - 4.35 C_{S,L}|^2. \tag{11}$$

This decay is not measured yet. However, based on the precisely measured lifetime of the B_c meson [92], a theoretical constraint on maximally allowed ${\rm BR}(B_c \to \tau\nu)$ can be obtained [93]. Recent estimates [90,94] suggest that ${\rm BR}(B_c \to \tau\nu)$ as large as 60% to 63% is still possible.

In our analysis we have not considered the constraint from the differential decay distributions of $B \to D^{(*)}\tau\bar{\nu}$ [3,6], which are known to be sensitive to scalar NP [95–97]. Compared to ratios $R_{D^{(*)}}$, the decay distributions are quite sensitive to hadronic form factors and parametric (e.g., V_{cb}) uncertainties. Furthermore, the corresponding experimental analyses [3,6] are model dependent and require the NP model's contributions to the background and the signal efficiency in order to obtain the data. Also, since the correlations among different data bins are not available, a combined data analysis is difficult. The improved measurements at Belle II [98] will be helpful in overcoming these issues (e.g., see discussion in Ref. [95]).

[5]Similar formulas are also given in Refs. [90,91].

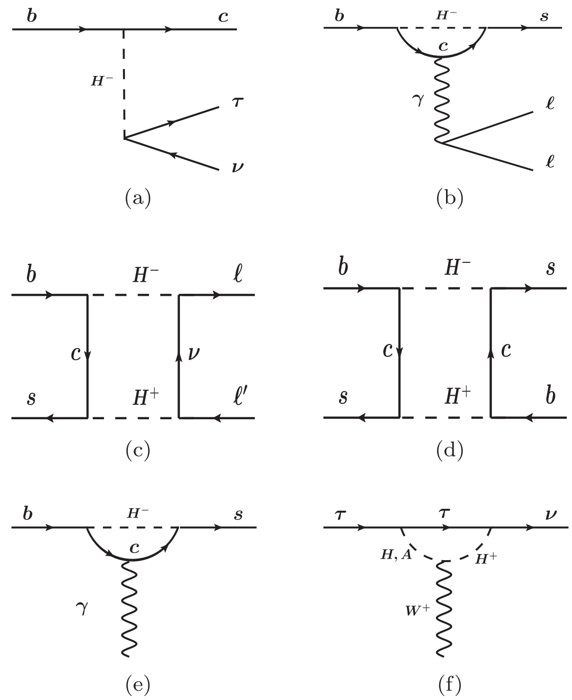

FIG. 1. Feynman diagrams for $b \to c\tau\bar{\nu}$ (a), $b \to s\ell^+\ell^-$ (b),(c), $B_s - \bar{B}_s$ mixing (d), $b \to s\gamma$ (e), and W-τ-ν vertex (f).

B. $b \to s\ell^+\ell^-$

The H^+ contributions to $b \to s\ell^+\ell^-$ processes have been discussed in several works (for example, see [69,70,99,100]), most of which have focused on top quark-H^+ loop diagrams. Such contributions, which are local in the effective field theory at scale $\mu \sim m_b$, are not present in our setup [see Eq. (6)]. Instead, the typical $b \to s\ell^+\ell^-$ contributions arise from the diagrams involving a charm quark in the loop as shown in Figs. 1(b) and 1(c).

The leading contribution to $b \to s\ell^+\ell^-$ comes from the penguin diagram in Fig. 1(b). This contribution in the effective field theory can be obtained via the penguin insertion of the four-quark operator $(\bar{c}_R b_L)(\bar{s}_L c_R)$ mediating the $b \to sc\bar{c}$ transition. This four-quark operator is generated at tree level via a diagram similar to Fig. 1(a) with the $\bar{\tau}\nu H^+$ vertex replaced by $\bar{s}cH^+$. For convenience we make use of a Fierz identity and define the following $b \to sc\bar{c}$ effective Hamiltonian

$$-\mathcal{H}_{\rm eff} = \frac{4G_F}{\sqrt{2}} V_{tb}V^*_{ts}\tilde{C}_{V,LR}(\bar{s}^\alpha_L\gamma^\mu b^\beta_L)(\bar{c}^\beta_R\gamma_\mu c^\alpha_R), \tag{12}$$

where α, β are the color indices, and the coefficient $\tilde{C}_{V,LR}$ at scale $\mu \sim m_{H^+}$ is given as $\tilde{C}_{V,LR} = -v^2|\rho_{tc}|^2/4m^2_{H^+}$. Then, closing the charm loop of the $b \to sc\bar{c}$ operator in Eq. (12) [diagram shown in Fig. 1(b) with H^+ integrated out] effects a nonlocal NP contribution to the vector operator $(\bar{s}_L\gamma_\mu b_L)(\bar{\ell}\gamma^\mu\ell)$. Adapting the results of Refs. [101,102]

to our case, we obtain the following NP contribution to the $b \to s\ell^+\ell^-$ Wilson coefficient[6]

$$C_{9\ell}(q^2,\mu) = \left[\frac{4}{9} + h(q^2, m_c, \mu)\right]\tilde{C}_{V,LR}, \qquad (13)$$

where the function $h(q^2, m_c)$ is given in Eq. (11) of Ref. [105]. Equation (13) gives a sufficiently accurate result[7] if the coefficient $\tilde{C}_{V,LR}$ arises at a scale close to the B-meson scale. However, since in our model the four-quark operator is generated at higher scale $\mu \sim m_{H^+}$, the renormalization group running effects are important. Therefore, instead of Eq. (13), we use the Wilson package [106] (which is based on the results of Refs. [107–114]), accounting for one-loop renormalization group evolution of $\tilde{C}_{V,LR}(\mu)$, to evaluate the mixing into $C_{9\ell}(\mu_b)$. Numerically, taking the NP scale $\mu_{\rm high} = 200$ GeV as an example case, we find $C_{9\ell}(\mu_b = 4.8\ {\rm GeV}) = 5.17\tilde{C}_{V,LR}(\mu_{\rm high})$. The Z-penguin diagram [Fig. 1(b) with $\gamma \to Z$] can be ignored as the corresponding loop function vanishes in the $m_c \to 0$ limit.

Another contribution to $b \to s\ell^+\ell^-$ comes from the box diagram in Fig. 1(c), which gives [99]

$$C_{9\tau}^{\rm NP} = C_{10\tau}^{\rm NP} = -\frac{v^2}{64\pi\alpha_e m_{H^+}^2}|\rho_{tc}\rho_{\tau\tau}|^2. \qquad (14)$$

The contributions in Eq. (13) are lepton flavor universal (due to $\gamma\ell\ell$ vertex). On the other hand, the contribution in Eq. (14) in principle introduces τ vs e, μ violation in our setup. However, this contribution depends on coupling product $|\rho_{tc}\rho_{\tau\tau}|$ that, as we will see later, is strongly constrained by the $b \to c\tau\bar{\nu}$ processes (and by demanding a solution to the $R_{D^{(*)}}$ anomaly), causing contributions in Eq. (14) to be completely negligible in the relevant parameter space. Consequently, NP contributions to $b \to s\ell^+\ell^-$ are practically described by Eq. (13) and universal to all lepton flavors. As a result, in our setup the ratios $R_{K^{(*)}}$ are SM-like in agreement with the observations made by the LHCb [33,34]. Equally important to note is that since NP contributions to Wilson coefficients ($C_{10\ell}$), related to axial-vector current, are negligible, the rate of the rare decay $B_s \to \mu^+\mu^-$ remain SM-like, which is also consistent with the new CMS result [115] based on 2016–2018 data corresponding to integrated luminosity of 140 fb^{-1}. The recent global fit to $b \to s\ell^+\ell^-$ data [excluding $R_{K^{(*)}}$ and BR$(B_s \to \mu^+\mu^-)$, which anyway remain unaffected in the considered scenario] shows that the NP scenario [116]

$$C_{9\ell} = -0.95 \pm 0.13 \qquad (15)$$

is strongly favored over the no NP hypothesis, corresponding to the 6.1σ pull away from the SM (for other NP scenarios, see Refs. [117,118][8]). In our analysis, we will use Eq. (15) to explain the current $b \to s\ell^+\ell^-$ discrepancies.

There are few important flavor constraints on ρ_{tc}. The most stringent constraint comes from the mass difference (ΔM_{B_s}) in $B_s - \bar{B}_s$ mixing. The H^+-induced box diagram (diagram with W^+ and H^+ in loop vanishes in the $m_c \to 0$ limit), shown in Fig. 1(d), gives rise to the effective Hamiltonian, $\mathcal{H}_{\rm eff} = C_{bs}(\bar{s}\gamma^\mu Lb)(\bar{s}\gamma^\mu Lb)$, where

$$C_{bs} = \frac{V_{ts}^{*2}V_{tb}^2|\rho_{tc}|^4}{128\pi^2 m_{H^+}^2}. \qquad (16)$$

The current value of the mass differences is $\Delta M_{B_s} = 17.741 \pm 0.020$ ps^{-1} [92], which is to be compared with the SM prediction $\Delta M_{B_s} = 18.4^{+0.7}_{-1.2}$ ps^{-1} [129].

Another relevant constraint arises from the radiative decay $B \to X_s\gamma$, which gets modified due to the loop diagram shown in Fig. 1(e). The corresponding dipole coefficient C_7 at scale $\mu \sim m_{H^+}$ at the leading order is given by [99]

$$C_7 = -\frac{7}{36}\frac{v^2}{4m_{H^+}^2}|\rho_{tc}|^2, \qquad (17)$$

while the coefficient related to $b \to sg$ is $C_8 \simeq (6/7)C_7$. The current experimental value for the branching ratio of $B \to X_s\gamma$ is $(3.32 \pm 0.15) \times 10^{-4}$ [2].

There are H^+ contributions to $K - \bar{K}$ mixing parameters ε_K and ΔM_K. The corresponding contributions arise from the box diagram shown in Fig. 1(d) after replacing external quarks $\{bs\} \to \{sd\}$. We calculate the NP contribution to $K - \bar{K}$ mixing following Ref. [130] and use experimental values from Ref. [92]; the resulting constraint however turns out to be weaker than those from B physics.

C. Shift in M_W

As mentioned in Introduction, the CDF value of M_W differs from the corresponding SM prediction by 7σ. This difference can be attributed to a NP correction to T parameter in the 2HDM (see, e.g., Refs. [131–145]). The SM value of M_W is calculable as [133]

$$M_W^2 = \frac{M_Z^2}{2}\left(1 + \sqrt{1 - \frac{4\pi\alpha_e(1+\Delta r)}{\sqrt{2}G_F M_Z^2}}\right), \qquad (18)$$

where Δr contains quantum corrections associated with oblique parameters and renormalization of α_e. Within the SM, $(\Delta r)_{\rm SM} \simeq 0.038$ [133]. Assuming that modifications in Δr arise from a NP contribution to T parameter, one can

[6]We follow notation of Ref. [103] for the $b \to s$ operator basis [104].

[7]The dominant contribution comes from q^2-independent terms in $h(q^2, m_c, \mu)$ (see, e.g., Ref. [101]).

[8]For fits before the new $R_{K^{(*)}}$ measurements, see Refs. [119–128].

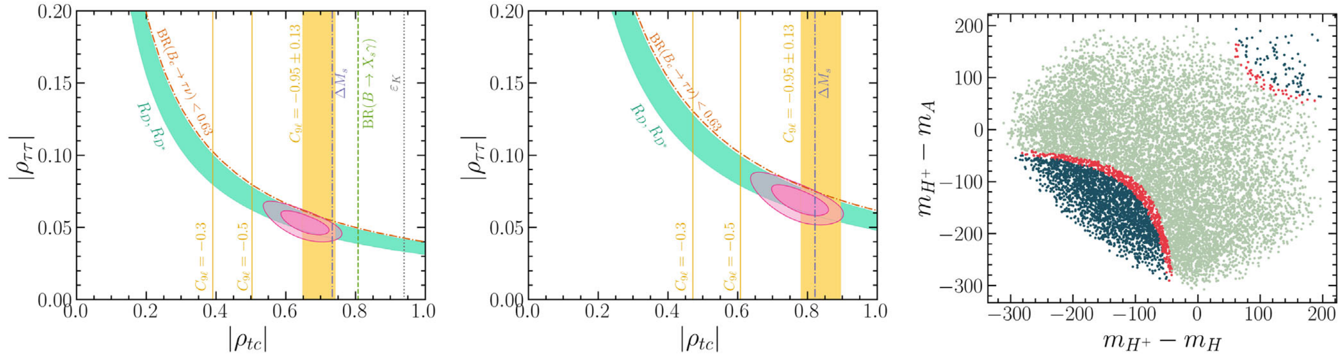

FIG. 2. First and second plots show results of fits to R_D and R_{D^*} (1σ) and $b \to s\ell^+\ell^-$ (1σ) for $m_{H^+} = 200$ GeV and 250 GeV, respectively. The dark and light magenta color contours are the global 1σ and 2σ allowed regions. The third plot shows the results of the parameter scan where the red points correspond to M_W values that are within 1σ of Eq. (2). See the text for other details.

parametrize NP effects as $\Delta r = (\Delta r)_{\rm SM} - (c_W^2/s_W^2)\alpha_e(M_Z)T$, where T in 2HDM is given by

$$T = \frac{1}{16\pi^2\alpha_e(M_Z)v^2}\{F(m_{H^+}^2, m_H^2) + F(m_{H^+}^2, m_A^2) - F(m_H^2, m_A^2)\}, \tag{19}$$

with loop function

$$F(a,b) = \frac{a+b}{2} - \frac{ab}{a-b}\log\frac{a}{b}. \tag{20}$$

Note that $F(a,b)$ vanishes in the limit of $a \to b$, indicating that at least two of the scalar states should have different masses in order to obtain a nonzero contribution to the T parameter. In our setup, the allowed range of m_{H^+} is fixed from seeking a solution to $R_{D^{(*)}}$ and $b \to s\ell^+\ell^-$ anomalies. The values of m_H and m_A then can be obtained from Eq. (4), with the quartic couplings Λ_4, Λ_5 varied within perturbative limits. We also include a NP contribution arising from S parameters following Ref. [133]; however these contributions are subdominant.

If m_H, m_A, and m_{H^+} are not equal, which is the case to obtain a finite T parameter as discussed above, then the vertex W-τ-ν_τ correction diagram in Fig. 1(f) gives a constraint on $\rho_{\tau\tau}$ coupling. This correction is sensitive to the mass splitting of physical scalars in 2HDM and can be parametrized by writing gauge coupling $g_{W\tau\nu} \to g_{W\tau\nu}(1+\delta g)$, where δg is

$$\delta g = \frac{|\rho_{\tau\tau}|^2}{32\pi^2} I(m_H^2/m_{H^\pm}^2, m_A^2/m_{H^\pm}^2), \tag{21}$$

with loop function $I(x,y)$ given by [146,147]

$$I(x,y) = 1 + \frac{1}{4}\frac{1+x}{1-x}\log x + \frac{1}{4}\frac{1+y}{1-y}\log y. \tag{22}$$

Note that the function $I(x,y)$ vanishes in the combined limit $x \to 1$ and $y \to 1$. The correction δg modifies leptonic decay rate of τ as $\Gamma_{\tau\to\ell\nu_\tau\bar{\nu}_\ell} \to \Gamma^{\rm SM}_{\tau\to\ell\nu_\tau\bar{\nu}_\ell}(1+2\delta g)$. The LFU test in τ decays is then given by $g_\tau/g_e = 1 + \delta g$, which is to be compared with the HFLAV value $g_\tau/g_e = 1.0029 \pm 0.0014$ [2]. We note that the $\rho_{\tau\tau}$ needed in our setup is very small (see next section), rendering δg to be completely negligible $\sim\mathcal{O}(10^{-5})$. The smallness of $\rho_{\tau\tau}$ also guarantees that the NP correction (calculated using the formula given in Ref. [67]) to the partial leptonic width of $Z \to \tau\tau$ is also negligible.

IV. RESULTS

In our numerical analysis, theoretical predictions of the flavor observables are obtained using FLAVIO [148]. Our main results are shown in Fig. 2. In the first plot, we show results for $R_{D^{(*)}}$ and $b \to s\ell^+\ell^-$ together with relevant constraints in the ($|\rho_{tc}|$, $|\rho_{\tau\tau}|$) plane for $m_{H^+} = 200$ GeV. In the plot, the phase ϕ ($\equiv \arg(\rho_{tc}\rho_{\tau\tau})$)[9] is fixed by maximizing the global log-likelihood function[10] in the space of NP parameters. This is performed using IMINUIT [149,150], which gives the best fit values $|\rho_{tc}| = 0.659$, $\rho_{\tau\tau} = 0.052$, $\phi \simeq 2\pi/3$. The green band shows the region consistent (within 1σ) with the current data on R_D and R_{D^*}. The vertical yellow band corresponds to value $C_{9\ell} \sim -1$ [1σ range of Eq. (15), to be exact]. The individual 95% C.L. exclusion bounds from ΔM_{B_s}, BR($B \to X_s\gamma$), and ϵ_K are also shown as vertical lines. The constraint BR($B_c \to \tau\bar{\nu}$) < 0.63 is shown as a dash-dotted orange curve (sitting just on top of 1σ solution of $R_{D^{(*)}}$), which rules out the region above it. We note that the $R_{D^{(*)}}$ solution (green band) only constrains the product $|\rho_{tc}\rho_{\tau\tau}|$, so the sizes of individual couplings remain unresolved. Including the data on $b \to s\ell^+\ell^-$ decays, which are essentially sensitive to $|\rho_{tc}|$, a far better constraint on the parameter space is

[9]We take ρ_{tc} real so that ϕ corresponds to the phase of $\rho_{\tau\tau}$.

[10]We assume that experimental uncertainties follow Gaussian distribution, and for the BR($B_c \to \tau\bar{\nu}$) constraint we assume that it has a uniform probability within limits [0, 0.63] and zero elsewhere.

achievable. The contours in magenta color show the 1σ and 2σ region where both $R_{D^{(*)}}$ and $b \to s\ell^+\ell^-$ data can be explained together. We also show smaller values $C_{9\ell} = -0.5, -0.3$ as solid yellow lines, illustrating the impact of ρ_{tc} variation on NP in $b \to s\ell^+\ell^-$. In the second plot, we show the results for $m_{H^+} = 250$ GeV. The constraints from $B \to X_s\gamma$ and ε_K are relaxed and lie outside the plot range. The best fit point now reads $|\rho_{tc}| = 0.784$, $\rho_{\tau\tau} = 0.068$, and ϕ same as before. In this case we note that ΔM_{B_s} constraint (dash-dotted blue line) already covers most of the 1σ range of Eq. (15), but there is still some allowed region left. Our results therefore indicate that for $m_{H^+} > 250$ GeV it becomes difficult to obtain $C_{9\ell} = -1$, but smaller (but appreciable) values such as $C_{9\ell} \sim -0.5$ are still possible.

In the third plot, we show parameter scan in the plane of mass differences $m_{H^+} - m_H$ and $m_{H^+} - m_A$, where the red points corresponds to M_W values within 1σ of the CDF measurement [Eq. (2)]; the light (dark) green points show M_W values which are below (above) 1σ range. In our setup, as mentioned earlier, the prediction of M_W depends on m_{H^+} and quartic couplings Λ_4, Λ_5. To obtain scan results, we vary m_{H^+} uniformly in the range (180, 300 GeV) and Λ_4, Λ_5 in the range $(-\sqrt{4\pi}, \sqrt{4\pi})$. To select allowed points, we require $m_H^2, m_A^2 > 0$, and reject $m_{H,A} \leq 100$ GeV. We note that the significant population of red points is when both H, A are heavier than H^+. There are a few red points in the region when H^+ is heavier than both H, A. However, we do not find any solution when only one of the H, A is heavier or lighter than H^+; this is because in these corners of the parameter space, the NP correction to T parameter [Eq. (19)] is negative, whereas a positive correction is needed to obtain a positive shift in M_W value. In the special case $\Lambda_5 = 0$, the second relation in Eq. (4) implies $m_H = m_A$, which in Fig. 2 (right) corresponds to the positive diagonal. So, even though the parameter space is reduced a lot, a W-boson mass consistent with the CDF measurement can still be obtained. On the other hand, in the case of vanishing Λ_4, Eq. (4) gives $m_{H^+}^2 - m_H^2 = m_A^2 - m_{H^+}^2$, from which one can deduce that both H, A cannot be simultaneously heavier or lighter than H^+, and therefore from the arguments presented above we find that the CDF value of M_W will not be explained in this case.

V. CONCLUSIONS

At present there are hints of LFU violation in $b \to c\ell\bar{\nu}$ data, reinforced further by the recent LHCb result on the combined measurement of R_D and R_{D^*}. On the other hand, no such effect is seen in $b \to s\ell^+\ell^-$, and LFU ratios $R_{K^{(*)}}$ are now SM-like. However, the discrepancies in the branching fractions and optimized observables related to $b \to s\ell^+\ell^-$ decays still remain. In this article we show that a H^+ boson, of few hundred GeV mass, can simultaneously explain anomalies in $R_{D^{(*)}}$ and $b \to s\ell^+\ell^-$ data. That a H^+ boson can explain the former is already known in literature. Here we uncover a nice correlation between H^+ effects in the charged- and neutral-current B decays: the enhanced rates of $B \to D^{(*)}\tau\bar{\nu}$ imply a destructive NP contribution in the Wilson coefficient $C_{9\ell}$. We show that the current constraints allow for $C_{9\ell} \sim -1$, a preferred solution to address discrepancies in the $b \to s\ell^+\ell^-$ decays. Additionally, we also show that the discrepancy observed in M_W by CDF II can also be explained by allowing the splitting among the physical scalars masses; the solution prefers the neutral states H, A heavier than H^+.

ACKNOWLEDGMENTS

I would like to thank Namit Mahajan for a useful conversation and his inputs on the manuscript, and Monika Blanke and Teppei Kitahara for helpful communication regarding their work on charged-current B decays. I also thank Manu George for reading the paper carefully. For diagrams and figures in paper, I acknowledge using JaxoDraw [151] and Matplotlib [152]. This research work is supported by Grant No. NSTC 111-2639-M-002-002-ASP of Taiwan.

APPENDIX: SCALAR POTENTIAL AND MASS SPECTRUM

Here we provide details about the scalar potential of a general 2HDM and the relations of its parameters with the masses of the scalars in the model. With H_1, H_2 denoting Higgs doublets, the scalar potential is given by [80]

$$\begin{aligned} V(H_1, H_2) &= M_{11}^2|H_1|^2 + M_{22}^2|H_2|^2 - (M_{12}^2 H_1^\dagger H_2 + \text{H.c.}) \\ &\quad + \frac{\Lambda_1}{2}|H_1|^4 + \frac{\Lambda_2}{2}|H_2|^4 + \Lambda_3|H_1|^2|H_2|^2 \\ &\quad + \Lambda_4|H_1^\dagger H_2|^2 + \bigg\{\frac{\Lambda_5}{2}(H_1^\dagger H_2)^2 + [\Lambda_6|H_1|^2 \\ &\quad + \Lambda_7|H_2|^2]H_1^\dagger H_2 + \text{H.c.}\bigg\}, \end{aligned} \tag{A1}$$

where parameters M_{12}^2, Λ_i ($i = 5, 6, 7$) in general can have complex phases. In this paper, we have taken $V(H_1, H_2)$ to be CP invariant for simplicity, and therefore all the potential parameters are real.

Working in the Higgs basis [153–155] where only one of the Higgs doublets receives a vacuum expectation value, we define doublets H_1, H_2 as

$$\begin{aligned} H_1 &= \begin{pmatrix} G^+ \\ \frac{1}{\sqrt{2}}(v + H_1^0 + iG^0) \end{pmatrix}, \\ H_2 &= \begin{pmatrix} H^+ \\ \frac{1}{\sqrt{2}}(H_2^0 + iA) \end{pmatrix}, \end{aligned} \tag{A2}$$

so that $\langle H_1\rangle = v/\sqrt{2}$ and $\langle H_2\rangle = 0$. In the above notation, G^+, G^0 are the goldstone bosons, H^+ and A are the charged scalar and CP-odd scalar, respectively, while the physical CP-even neutral scalars h and H are given by

$$h = H_1^0 \sin\gamma + H_2^0 \cos\gamma,$$
$$H = H_1^0 \cos\gamma - H_2^0 \sin\gamma, \tag{A3}$$

with γ denoting the h-H mixing angle [analogous to $(\beta-\alpha)$ in type-II 2HDM notation].

Minimization of the potential gives conditions: $M_{11}^2 + \Lambda_1(v^2/2) = 0$, $M_{12}^2 - \Lambda_6(v^2/2) = 0$. The relations between potential parameters and the scalar masses, which we are mainly interested in, are given as [80]

$$m_{H+}^2 = M_{22}^2 + \frac{v^2}{2}\Lambda_3, \tag{A4}$$

$$m_A^2 - m_{H+}^2 = -\frac{v^2}{2}(\Lambda_5 - \Lambda_4), \tag{A5}$$

$$m_H^2 + m_h^2 - m_A^2 = v^2(\Lambda_1 + \Lambda_5), \tag{A6}$$

$$(m_H^2 - m_h^2)^2 = [m_A^2 + (\Lambda_5 - \Lambda_1)v^2]^2 + 4\Lambda_6^2 v^4, \tag{A7}$$

$$\sin\gamma\cos\gamma = -\frac{\Lambda_6 v^2}{m_H^2 - m_h^2}. \tag{A8}$$

In case of very small mixing angle, i.e., $\cos\gamma \to 0$, which we have taken in this paper, the simplified relations for the scalar masses are $m_h^2 \simeq \Lambda_1 v^2$, $m_A^2 = M_{22}^2 + (v^2/2)(\Lambda_3 + \Lambda_4 - \Lambda_5)$, and the ones given in Eq. (4).

[1] First joint measurement of $R(D^*)$ and $R(D^0)$ at LHCb, https://indico.cern.ch/event/1187939/.

[2] Yasmine Sara Amhis *et al.* (HFLAV Collaboration), Averages of b-hadron, c-hadron, and τ-lepton properties as of 2018, Eur. Phys. J. C **81**, 226 (2021).

[3] J. P. Lees *et al.* (*BABAR* Collaboration), Measurement of an excess of $\bar{B} \to D^{(*)}\tau^-\bar{\nu}_\tau$ decays and implications for charged Higgs bosons, Phys. Rev. D **88**, 072012 (2013).

[4] J. P. Lees *et al.* (*BABAR* Collaboration), Evidence for an Excess of $\bar{B} \to D^{(*)}\tau^-\bar{\nu}_\tau$ Decays, Phys. Rev. Lett. **109**, 101802 (2012).

[5] S. Hirose *et al.* (Belle Collaboration), Measurement of the τ Lepton Polarization and $R(D^*)$ in the Decay $\bar{B} \to D^*\tau^-\bar{\nu}_\tau$, Phys. Rev. Lett. **118**, 211801 (2017).

[6] M. Huschle *et al.* (Belle Collaboration), Measurement of the branching ratio of $\bar{B} \to D^{(*)}\tau^-\bar{\nu}_\tau$ relative to $\bar{B} \to D^{(*)}\ell^-\bar{\nu}_\ell$ decays with hadronic tagging at Belle, Phys. Rev. D **92**, 072014 (2015).

[7] G. Caria *et al.* (Belle Collaboration), Measurement of $\mathcal{R}(D)$ and $\mathcal{R}(D^*)$ with a Semileptonic Tagging Method, Phys. Rev. Lett. **124**, 161803 (2020).

[8] Roel Aaij *et al.* (LHCb Collaboration), Measurement of the Ratio of Branching Fractions $\mathcal{B}(\bar{B}^0 \to D^{*+}\tau^-\bar{\nu}_\tau)/\mathcal{B}(\bar{B}^0 \to D^{*+}\mu^-\bar{\nu}_\mu)$, Phys. Rev. Lett. **115**, 111803 (2015); **115**, 159901(E) (2015).

[9] R. Aaij *et al.* (LHCb Collaboration), Measurement of the Ratio of the $B^0 \to D^{*-}\tau^+\nu_\tau$ and $B^0 \to D^{*-}\mu^+\nu_\mu$ Branching Fractions using Three-Prong τ-Lepton Decays, Phys. Rev. Lett. **120**, 171802 (2018).

[10] R. Aaij *et al.* (LHCb Collaboration), Test of lepton flavor universality by the measurement of the $B^0 \to D^{*-}\tau^+\nu_\tau$ branching fraction using three-prong τ decays, Phys. Rev. D **97**, 072013 (2018).

[11] Dante Bigi and Paolo Gambino, Revisiting $B \to D\ell\nu$, Phys. Rev. D **94**, 094008 (2016).

[12] Paolo Gambino, Martin Jung, and Stefan Schacht, The V_{cb} puzzle: An update, Phys. Lett. B **795**, 386 (2019).

[13] Marzia Bordone, Martin Jung, and Danny van Dyk, Theory determination of $\bar{B} \to D^{(*)}\ell^-\bar{\nu}$ form factors at $\mathcal{O}(1/m_c^2)$, Eur. Phys. J. C **80**, 74 (2020).

[14] Florian U. Bernlochner, Zoltan Ligeti, Michele Papucci, and Dean J. Robinson, Combined analysis of semileptonic B decays to D and D^*: $R(D^{(*)})$, $|V_{cb}|$, and new physics, Phys. Rev. D **95**, 115008 (2017); **97**, 059902(E) (2018).

[15] Sneha Jaiswal, Soumitra Nandi, and Sunando Kumar Patra, Extraction of $|V_{cb}|$ from $B \to D^{(*)}\ell\nu_\ell$ and the Standard Model predictions of $R(D^{(*)})$, J. High Energy Phys. 12 (2017) 060.

[16] G. Martinelli, S. Simula, and L. Vittorio, $|V_{cb}|$ and $R(D)^{(*)}$) using lattice QCD and unitarity, Phys. Rev. D **105**, 034503 (2022).

[17] Dante Bigi, Paolo Gambino, and Stefan Schacht, $R(D^*)$, $|V_{cb}|$, and the heavy quark symmetry relations between form factors, J. High Energy Phys. 11 (2017) 061.

[18] A. Bazavov *et al.* (Fermilab Lattice, MILC Collaborations), Semileptonic form factors for $B \to D^*\ell\nu$ at nonzero recoil from 2 + 1-flavor lattice QCD, Eur. Phys. J. C **82**, 1141 (2022).

[19] R. Aaij *et al.* (LHCb Collaboration), Measurement of the Ratio of Branching Fractions $\mathcal{B}(B_c^+ \to J/\psi\tau^+\nu_\tau)/\mathcal{B}(B_c^+ \to J/\psi\mu^+\nu_\mu)$, Phys. Rev. Lett. **120**, 121801 (2018).

[20] R. Aaij *et al.* (LHCb Collaboration), Observation of the Decay $\Lambda_b^0 \to \Lambda_c^+\tau^-\bar{\nu}_\tau$, Phys. Rev. Lett. **128**, 191803 (2022).

[21] Marco Fedele, Monika Blanke, Andreas Crivellin, Syuhei Iguro, Teppei Kitahara, Ulrich Nierste, and Ryoutaro Watanabe, Impact of $\Lambda_b \to \Lambda_c\tau\nu$ measurement on new

physics in $b \to cl\nu$ transitions, Phys. Rev. D **107**, 055005 (2023).

[22] R. Glattauer *et al.* (Belle Collaboration), Measurement of the decay $B \to D\ell\nu_\ell$ in fully reconstructed events and determination of the Cabibbo-Kobayashi-Maskawa matrix element $|V_{cb}|$, Phys. Rev. D **93**, 032006 (2016).

[23] A. Abdesselam *et al.* (Belle Collaboration), Precise determination of the CKM matrix element $|V_{cb}|$ with $\bar{B}^0 \to D^{*+}\ell^-\bar{\nu}_\ell$ decays with hadronic tagging at Belle, arXiv:1702.01521.

[24] E. Waheed *et al.* (Belle Collaboration), Measurement of the CKM matrix element $|V_{cb}|$ from $B^0 \to D^{*-}\ell^+\nu_\ell$ at Belle, Phys. Rev. D **100**, 052007 (2019); **103**, 079901(E) (2021).

[25] R Aaij *et al.* (LHCb Collaboration), Measurement of Form-Factor-Independent Observables in the Decay $B^0 \to K^{*0}\mu^+\mu^-$, Phys. Rev. Lett. **111**, 191801 (2013).

[26] Roel Aaij *et al.* (LHCb Collaboration), Angular analysis of the $B^0 \to K^{*0}\mu^+\mu^-$ decay using 3 fb^{-1} of integrated luminosity, J. High Energy Phys. 02 (2016) 104.

[27] Roel Aaij *et al.* (LHCb Collaboration), Measurement of CP-Averaged Observables in the $B^0 \to K^{*0}\mu^+\mu^-$ Decay, Phys. Rev. Lett. **125**, 011802 (2020).

[28] Roel Aaij *et al.* (LHCb Collaboration), Angular analysis and differential branching fraction of the decay $B_s^0 \to \phi\mu^+\mu^-$, J. High Energy Phys. 09 (2015) 179.

[29] Roel Aaij *et al.* (LHCb Collaboration), Angular analysis of the rare decay $B_s^0 \to \phi\mu^+\mu^-$, J. High Energy Phys. 11 (2021) 043.

[30] Roel Aaij *et al.* (LHCb Collaboration), Branching Fraction Measurements of the Rare $B_s^0 \to \phi\mu^+\mu^-$ and $B_s^0 \to f_2'(1525)\mu^+\mu^-$- Decays, Phys. Rev. Lett. **127**, 151801 (2021).

[31] R. Aaij *et al.* (LHCb Collaboration), Differential branching fractions and isospin asymmetries of $B \to K^{(*)}\mu^+\mu^-$ decays, J. High Energy Phys. 06 (2014) 133.

[32] Roel Aaij *et al.* (LHCb Collaboration), Differential branching fraction and angular analysis of $\Lambda_b^0 \to \Lambda\mu^+\mu^-$ decays, J. High Energy Phys. 06 (2015) 115; 09 (2018) 145(E).

[33] LHCb Collaboration, Test of lepton universality in $b \to s\ell^+\ell^-$ decays, arXiv:2212.09152.

[34] LHCb Collaboration, Measurement of lepton universality parameters in $B^+ \to K^+\ell^+\ell^-$ and $B^0 \to K^{*0}\ell^+\ell^-$ decays, arXiv:2212.09153.

[35] Gudrun Hiller and Frank Kruger, More model-independent analysis of $b \to s$ processes, Phys. Rev. D **69**, 074020 (2004).

[36] Marzia Bordone, Gino Isidori, and Andrea Pattori, On the Standard Model predictions for R_K and R_{K^*}, Eur. Phys. J. C **76**, 440 (2016).

[37] Gino Isidori, Saad Nabeebaccus, and Roman Zwicky, QED corrections in $\bar{B} \to \bar{K}\ell^+\ell^-$ at the double-differential level, J. High Energy Phys. 12 (2020) 104.

[38] Gino Isidori, Davide Lancierini, Saad Nabeebaccus, and Roman Zwicky, QED in $\bar{B} \to \bar{K}\ell^+\ell^-$ LFU ratios: Theory versus experiment, a Monte Carlo study, J. High Energy Phys. 10 (2022) 146.

[39] R. Aaij *et al.* (LHCb Collaboration), Test of lepton universality with $B^0 \to K^{*0}\ell^+\ell^-$ decays, J. High Energy Phys. 08 (2017) 055.

[40] Roel Aaij *et al.* (LHCb Collaboration), Search for Lepton-Universality Violation in $B^+ \to K^+\ell^+\ell^-$ Decays, Phys. Rev. Lett. **122**, 191801 (2019).

[41] Roel Aaij *et al.* (LHCb Collaboration), Test of lepton universality in beauty-quark decays, Nat. Phys. **18**, 277 (2022).

[42] Joaquim Matias, Federico Mescia, Marc Ramon, and Javier Virto, Complete Anatomy of $\bar{B}_d -> \bar{K}^{*0}(->K\pi)l^+l^-$ and its angular distribution, J. High Energy Phys. 04 (2012) 104.

[43] Diganta Das and Rahul Sinha, New physics effects and hadronic form factor uncertainties in $B \to K^*\ell^+\ell^-$, Phys. Rev. D **86**, 056006 (2012).

[44] Sebastien Descotes-Genon, Tobias Hurth, Joaquim Matias, and Javier Virto, Optimizing the basis of $B \to K^*ll$ observables in the full kinematic range, J. High Energy Phys. 05 (2013) 137.

[45] Ronald R. Horgan, Zhaofeng Liu, Stefan Meinel, and Matthew Wingate, Lattice QCD calculation of form factors describing the rare decays $B \to K^*\ell^+\ell^-$ and $B_s \to \phi\ell^+\ell^-$, Phys. Rev. D **89**, 094501 (2014).

[46] Frederik Beaujean, Christoph Bobeth, and Danny van Dyk, Comprehensive Bayesian analysis of rare (semi)leptonic and radiative B decays, Eur. Phys. J. C **74**, 2897 (2014); **74**, 3179(E) (2014).

[47] Rusa Mandal, Rahul Sinha, and Diganta Das, Testing new physics effects in $B \to K^*\ell^+\ell^-$, Phys. Rev. D **90**, 096006 (2014).

[48] James Lyon and Roman Zwicky, Resonances gone topsy turvy—the charm of QCD or new physics in $b \to s\ell^+\ell^-$? arXiv:1406.0566.

[49] Sebastian Jäger and Jorge Martin Camalich, Reassessing the discovery potential of the $B \to K^*\ell^+\ell^-$ decays in the large-recoil region: SM challenges and BSM opportunities, Phys. Rev. D **93**, 014028 (2016).

[50] Marco Ciuchini, Marco Fedele, Enrico Franco, Satoshi Mishima, Ayan Paul, Luca Silvestrini, and Mauro Valli, $B \to K^*\ell^+\ell^-$ decays at large recoil in the Standard Model: A theoretical reappraisal, J. High Energy Phys. 06 (2016) 116.

[51] Marco Ciuchini, Marco Fedele, Enrico Franco, Ayan Paul, Luca Silvestrini, and Mauro Valli, Charming penguins and lepton universality violation in $b \to s\ell^+\ell^-$ decays, Eur. Phys. J. C **83**, 64 (2023).

[52] Nico Gubernari, Danny van Dyk, and Javier Virto, Non-local matrix elements in $B_{(s)} \to \{K^{(*)}.\phi\}\ell^+\ell^-$, J. High Energy Phys. 02 (2021) 088.

[53] Nico Gubernari, Méril Reboud, Danny van Dyk, and Javier Virto, Improved theory predictions and global analysis of exclusive $b \to s\mu^=\mu^-$ processes, J. High Energy Phys. 09 (2022) 133.

[54] T. Aaltonen *et al.* (CDF Collaboration), High-precision measurement of the W boson mass with the CDF II detector, Science **376**, 170 (2022).

[55] M. Awramik, M. Czakon, A. Freitas, and G. Weiglein, Precise prediction for the W boson mass in the standard model, Phys. Rev. D **69**, 053006 (2004).

[56] Morad Aaboud *et al.* (ATLAS Collaboration), Measurement of the W-boson mass in pp collisions at $\sqrt{s} = 7$ TeV with the ATLAS detector, Eur. Phys. J. C **78**, 110 (2018); **78**, 898(E) (2018).

[57] Roel Aaij *et al.* (LHCb Collaboration), Measurement of the W boson mass, J. High Energy Phys. 01 (2022) 036.
[58] Triparno Bandyopadhyay, Ankita Budhraja, Samadrita Mukherjee, and Tuhin S. Roy, A twisted tale of the transverse-mass tail, arXiv:2212.02534.
[59] T. D. Lee, A theory of spontaneous T violation, Phys. Rev. D **8**, 1226 (1973).
[60] Andreas Crivellin, Christoph Greub, and Ahmet Kokulu, Explaining $B \to D\tau\nu$, $B \to D^*\tau\nu$ and $B \to \tau\nu$ in a 2HDM of type III, Phys. Rev. D **86**, 054014 (2012).
[61] Alejandro Celis, Martin Jung, Xin-Qiang Li, and Antonio Pich, Sensitivity to charged scalars in $B \to D^{(*)}\tau\nu_\tau$ and $B \to \tau\nu$ decays, J. High Energy Phys. 01 (2013) 054.
[62] Minoru Tanaka and Ryoutaro Watanabe, New physics in the weak interaction of $\bar{B} \to D^{(*)}\tau\bar{\nu}$, Phys. Rev. D **87**, 034028 (2013).
[63] P. Ko, Yuji Omura, and Chaehyun Yu, $B \to D^{(*)}\tau\nu$ and $B \to \tau\nu$ in chiral $U(1)'$ models with flavored multi Higgs doublets, J. High Energy Phys. 03 (2013) 151.
[64] Andreas Crivellin, Ahmet Kokulu, and Christoph Greub, Flavor-phenomenology of two-Higgs-doublet models with generic Yukawa structure, Phys. Rev. D **87**, 094031 (2013).
[65] Andreas Crivellin, Julian Heeck, and Peter Stoffer, A Perturbed Lepton-Specific Two-Higgs-Doublet Model Facing Experimental Hints for Physics Beyond the Standard Model, Phys. Rev. Lett. **116**, 081801 (2016).
[66] C. S. Kim, Yeo Woong Yoon, and Xing-Bo Yuan, Exploring top quark FCNC within 2HDM type III in association with flavor physics, J. High Energy Phys. 12 (2015) 038.
[67] James M. Cline, Scalar doublet models confront τ and b anomalies, Phys. Rev. D **93**, 075017 (2016).
[68] Jong-Phil Lee, $B \to D^{(*)}\tau\nu_\tau$ in the 2HDM with an anomalous τ coupling, Phys. Rev. D **96**, 055005 (2017).
[69] Syuhei Iguro and Kazuhiro Tobe, $R(D^{(*)})$ in a general two Higgs doublet model, Nucl. Phys. **B925**, 560 (2017).
[70] Syuhei Iguro and Yuji Omura, Status of the semileptonic B decays and muon g-2 in general 2HDMs with right-handed neutrinos, J. High Energy Phys. 05 (2018) 173.
[71] Chuan-Hung Chen and Takaaki Nomura, Charged Higgs boson contribution to $B_q^- \to \ell\bar{\nu}$ and $\bar{B} \to (P,V)\ell\bar{\nu}$ in a generic two-Higgs doublet model, Phys. Rev. D **98**, 095007 (2018).
[72] R. Martinez, C. F. Sierra, and German Valencia, Beyond $\mathcal{R}(D^{(*)})$ with the general type-III 2HDM for $b \to c\tau\nu$, Phys. Rev. D **98**, 115012 (2018).
[73] Shao-Ping Li, Xin-Qiang Li, Ya-Dong Yang, and Xin Zhang, $R_{D^{(*)}}$, $R_{K^{(*)}}$ and neutrino mass in the 2HDM-III with right-handed neutrinos, J. High Energy Phys. 09 (2018) 149.
[74] Jonathan Cardozo, J. H. Muñoz, Nestor Quintero, and Eduardo Rojas, Analysing the charged scalar boson contribution to the charged-current B meson anomalies, J. Phys. G **48**, 035001 (2021).
[75] Peter Athron, Csaba Balazs, Tomás E. Gonzalo, Douglas Jacob, Farvah Mahmoudi, and Cristian Sierra, Likelihood analysis of the flavour anomalies and $g-2$ in the general two Higgs doublet model, J. High Energy Phys. 01 (2022) 037.
[76] Syuhei Iguro, Revival of H^- interpretation of $R_{D^{(*)}}$ anomaly and closing low mass window, Phys. Rev. D **105**, 095011 (2022).
[77] Monika Blanke, Syuhei Iguro, and Hantian Zhang, Towards ruling out the charged Higgs interpretation of the $R_{D^{(*)}}$ anomaly, J. High Energy Phys. 06 (2022) 043.
[78] Michael E. Peskin and Tatsu Takeuchi, Estimation of oblique electroweak corrections, Phys. Rev. D **46**, 381 (1992).
[79] G. C. Branco, P. M. Ferreira, L. Lavoura, M. N. Rebelo, Marc Sher, and Joao P. Silva, Theory and phenomenology of two-Higgs-doublet models, Phys. Rep. **516**, 1 (2012).
[80] Sacha Davidson and Howard E. Haber, Basis-independent methods for the two-Higgs-doublet model, Phys. Rev. D **72**, 035004 (2005); **72**, 099902(E) (2005).
[81] Farvah Mahmoudi and Oscar Stal, Flavor constraints on the two-Higgs-doublet model with general Yukawa couplings, Phys. Rev. D **81**, 035016 (2010).
[82] Albert M. Sirunyan *et al.* (CMS Collaboration), Combined measurements of Higgs boson couplings in proton–proton collisions at $\sqrt{s} = 13$ TeV, Eur. Phys. J. C **79**, 421 (2019).
[83] Georges Aad *et al.* (ATLAS Collaboration), Combined measurements of Higgs boson production and decay using up to 80 fb^{-1} of proton-proton collision data at $\sqrt{s} =$ 13 TeV collected with the ATLAS experiment, Phys. Rev. D **101**, 012002 (2020).
[84] Syuhei Iguro, Yuji Omura, and Michihisa Takeuchi, Test of the $R(D^{(*)})$ anomaly at the LHC, Phys. Rev. D **99**, 075013 (2019).
[85] Albert M. Sirunyan *et al.* (CMS Collaboration), Search for a W' boson decaying to a τ lepton and a neutrino in proton-proton collisions at $\sqrt{s} = 13$ TeV, Phys. Lett. B **792**, 107 (2019).
[86] Albert M. Sirunyan *et al.* (CMS Collaboration), Search for low mass vector resonances decaying into quark-antiquark pairs in proton-proton collisions at $\sqrt{s} = 13$ TeV, J. High Energy Phys. 01 (2018) 097.
[87] Morad Aaboud *et al.* (ATLAS Collaboration), Search for low-mass resonances decaying into two jets and produced in association with a photon using pp collisions at $\sqrt{s} =$ 13 TeV with the ATLAS detector, Phys. Lett. B **795**, 56 (2019).
[88] A. M. Sirunyan *et al.* (CMS Collaboration), Search for Narrow Resonances in the b-Tagged Dijet Mass Spectrum in Proton-Proton Collisions at $\sqrt{s} = 8$ TeV, Phys. Rev. Lett. **120**, 201801 (2018).
[89] Syuhei Iguro, Teppei Kitahara, and Ryoutaro Watanabe, Global fit to $b \to c\tau\nu$ anomalies 2022 mid-autumn, arXiv:2210.10751.
[90] Monika Blanke, Andreas Crivellin, Stefan de Boer, Teppei Kitahara, Marta Moscati, Ulrich Nierste, and Ivan Nišandžić, Impact of polarization observables and $B_c \to \tau\nu$ on new physics explanations of the $b \to c\tau\nu$ anomaly, Phys. Rev. D **99**, 075006 (2019).
[91] Syuhei Iguro, Teppei Kitahara, Yuji Omura, Ryoutaro Watanabe, and Kei Yamamoto, D* polarization vs. $R_{D^{(*)}}$ anomalies in the leptoquark models, J. High Energy Phys. 02 (2019) 194.

[92] R. L. Workman *et al.* (Particle Data Group), Review of particle physics, Prog. Theor. Exp. Phys. **2022**, 083C01 (2022).

[93] Rodrigo Alonso, Benjamín Grinstein, and Jorge Martin Camalich, Lifetime of B_c^- Constrains Explanations for Anomalies in $B \to D^{(*)}\tau\nu$, Phys. Rev. Lett. **118**, 081802 (2017).

[94] Jason Aebischer and Benjamín Grinstein, Standard Model prediction of the B_c lifetime, J. High Energy Phys. 07 (2021) 130.

[95] Yasuhito Sakaki, Minoru Tanaka, Andrey Tayduganov, and Ryoutaro Watanabe, Probing new physics with q^2 distributions in $\bar{B} \to D^{(*)}\tau\bar{\nu}$, Phys. Rev. D **91**, 114028 (2015).

[96] Marat Freytsis, Zoltan Ligeti, and Joshua T. Ruderman, Flavor models for $\bar{B} \to D^{(*)}\tau\bar{\nu}$, Phys. Rev. D **92**, 054018 (2015).

[97] Alejandro Celis, Martin Jung, Xin-Qiang Li, and Antonio Pich, Scalar contributions to $b \to c(u)\tau\nu$ transitions, Phys. Lett. B **771**, 168 (2017).

[98] W. Altmannshofer *et al.* (Belle-II Collaboration), The Belle II physics book, Prog. Theor. Exp. Phys. **2019**, 123C01 (2019); **2020**, 029201(E) (2020).

[99] Andreas Crivellin, Dario Müller, and Christoph Wiegand, $b \to s\ell^+\ell^-$ transitions in two-Higgs-doublet models, J. High Energy Phys. 06 (**2019**) 119.

[100] Peter Athron, Csaba Balazs, Tomas Gonzalo, Douglas Jacob, Farvah Mahmoudi, and Cristian Felipe Sierra Fonseca, Likelihood analysis of the general 2HDM with Gambit's FlavBit, Proc. Sci. CompTools2021 (**2022**) 011.

[101] Sebastian Jäger, Matthew Kirk, Alexander Lenz, and Kirsten Leslie, Charming new B-physics, J. High Energy Phys. 03 (2020) 122.

[102] Sebastian Jäger, Matthew Kirk, Alexander Lenz, and Kirsten Leslie, Charming new physics in rare B-decays and mixing?, Phys. Rev. D **97**, 015021 (2018).

[103] David London and Joaquim Matias, B Flavour anomalies: 2021 Theoretical status report, Annu. Rev. Nucl. Part. Sci. **72**, 37 (2022).

[104] Gerhard Buchalla, Andrzej J. Buras, and Markus E. Lautenbacher, Weak decays beyond leading logarithms, Rev. Mod. Phys. **68**, 1125 (1996).

[105] M. Beneke, T. Feldmann, and D. Seidel, Systematic approach to exclusive $B \to Vl^+l^-$, $V\gamma$ decays, Nucl. Phys. **B612**, 25 (2001).

[106] Jason Aebischer, Jacky Kumar, and David M. Straub, Wilson: A Python package for the running and matching of Wilson coefficients above and below the electroweak scale, Eur. Phys. J. C **78**, 1026 (2018).

[107] Elizabeth E. Jenkins, Aneesh V. Manohar, and Michael Trott, Renormalization group evolution of the standard model dimension six operators I: Formalism and lambda dependence, J. High Energy Phys. 10 (2013) 087.

[108] Elizabeth E. Jenkins, Aneesh V. Manohar, and Michael Trott, Renormalization group evolution of the standard model dimension six operators II: Yukawa dependence, J. High Energy Phys. 01 (**2014**) 035.

[109] Rodrigo Alonso, Elizabeth E. Jenkins, Aneesh V. Manohar, and Michael Trott, Renormalization group evolution of the standard model dimension six operators III: Gauge coupling dependence and phenomenology, J. High Energy Phys. 04 (2014) 159.

[110] Elizabeth E. Jenkins, Aneesh V. Manohar, and Peter Stoffer, Low-energy effective field theory below the electroweak scale: Operators and matching, J. High Energy Phys. 03 (2018) 016.

[111] Jason Aebischer, Matteo Fael, Christoph Greub, and Javier Virto, B physics beyond the standard model at one loop: Complete renormalization group evolution below the electroweak scale, J. High Energy Phys. 09 (2017) 158.

[112] Elizabeth E. Jenkins, Aneesh V. Manohar, and Peter Stoffer, Low-energy effective field theory below the electroweak scale: Anomalous dimensions, J. High Energy Phys. 01 (2018) 084.

[113] Alejandro Celis, Javier Fuentes-Martin, Avelino Vicente, and Javier Virto, DsixTools: The standard model effective field theory toolkit, Eur. Phys. J. C **77**, 405 (2017).

[114] Florian Herren and Matthias Steinhauser, Version 3 of RunDec and CRunDec, Comput. Phys. Commun. **224**, 333 (2018).

[115] Measurement of the $B_s^0 \to \mu^+\mu^-$ decay properties and search for the $B^0 \to \mu^+\mu^-$ decay in proton-proton collisions at $\sqrt{s} = 13$ TeV, arXiv:2212.10311.

[116] T. Hurth, F. Mahmoudi, D. Martinez Santos, and S. Neshatpour, Neutral current B-decay anomalies, in *8th Workshop on Theory, Phenomenology and Experiments in Flavour Physics: Neutrinos, Flavor Physics and Beyond* (Springer, Italy, 2022), arXiv:2210.07221.

[117] Admir Greljo, Jakub Salko, Aleks Smolkovič, and Peter Stangl, Rare b decays meet high-mass Drell-Yan, arXiv:2212.10497.

[118] Marco Ciuchini, Marco Fedele, Enrico Franco, Ayan Paul, Luca Silvestrini, and Mauro Valli, Constraints on lepton universality violation from rare B decays, Phys. Rev. D **107**, 055036 (2023).

[119] Ashutosh Kumar Alok, Amol Dighe, Shireen Gangal, and Dinesh Kumar, Continuing search for new physics in $b \to s\mu\mu$ decays: Two operators at a time, J. High Energy Phys. 06 (2019) 089.

[120] Alakabha Datta, Jacky Kumar, and David London, The B anomalies and new physics in $b \to se^+e^-$, Phys. Lett. B **797**, 134858 (2019).

[121] T. Hurth, F. Mahmoudi, D. Martinez Santos, and S. Neshatpour, More indications for lepton nonuniversality in $b \to s\ell^+\ell^-$, Phys. Lett. B **824**, 136838 (2022).

[122] Marcel Algueró, Bernat Capdevila, Sébastien Descotes-Genon, Joaquim Matias, and Martín Novoa-Brunet, $b \to s\ell^+\ell^-$ global fits after R_{K_S} and $R_{K^{*+}}$, Eur. Phys. J. C **82**, 326 (2022).

[123] Wolfgang Altmannshofer and Peter Stangl, New physics in rare B decays after Moriond 2021, Eur. Phys. J. C **81**, 952 (2021).

[124] Marco Ciuchini, Marco Fedele, Enrico Franco, Ayan Paul, Luca Silvestrini, and Mauro Valli, Lessons from the $B^{0,+} \to K^{*0,+}\mu^+\mu^-$ angular analyses, Phys. Rev. D **103**, 015030 (2021).

[125] Li-Sheng Geng, Benjamín Grinstein, Sebastian Jäger, Shuang-Yi Li, Jorge Martin Camalich, and Rui-Xiang Shi, Implications of new evidence for lepton-universality

violation in $b \to s\ell^+\ell^-$ decays, Phys. Rev. D **104**, 035029 (2021).
[126] Ashutosh Kumar Alok, Neetu Raj Singh Chundawat, Shireen Gangal, and Dinesh Kumar, A global analysis of $b \to s\ell\ell$ data in heavy and light Z' models, Eur. Phys. J. C **82**, 967 (2022).
[127] Neetu Raj Singh Chundawat, CP violation in $b \to s\ell\ell$: A model independent analysis, arXiv:2207.10613.
[128] Aritra Biswas, Soumitra Nandi, Sunando Kumar Patra, and Ipsita Ray, New physics in $b \to s\ell\ell$ decays with complex Wilson coefficients, Nucl. Phys. **B969**, 115479 (2021).
[129] Luca Di Luzio, Matthew Kirk, Alexander Lenz, and Thomas Rauh, ΔM_s theory precision confronts flavour anomalies, J. High Energy Phys. 12 (2019) 009.
[130] Wei-Shu Hou and Girish Kumar, Strange processes in general two Higgs doublet model, J. High Energy Phys. 10 (2022) 129.
[131] Henning Bahl, Johannes Braathen, and Georg Weiglein, New physics effects on the W-boson mass from a doublet extension of the SM Higgs sector, Phys. Lett. B **833**, 137295 (2022).
[132] Huayang Song, Wei Su, and Mengchao Zhang, Electroweak phase transition in 2HDM under Higgs, Z-pole, and W precision measurements, J. High Energy Phys. 10 (2022) 048.
[133] K. S. Babu, Sudip Jana, and Vishnu P. K., Correlating W-Boson Mass Shift with Muon $g-2$ in the Two Higgs Doublet Model, Phys. Rev. Lett. **129**, 121803 (2022).
[134] F. Arco, S. Heinemeyer, and M. J. Herrero, Sensitivity and constraints to the 2HDM soft-breaking Z_2 parameter m_{12}, Phys. Lett. B **835**, 137548 (2022).
[135] Soojin Lee, Kingman Cheung, Jinheung Kim, Chih-Ting Lu, and Jeonghyeon Song, Status of the two-Higgs-doublet model in light of the CDF m_W measurement, Phys. Rev. D **106**, 075013 (2022).
[136] Chih-Ting Lu, Lei Wu, Yongcheng Wu, and Bin Zhu, Electroweak precision fit and new physics in light of the W boson mass, Phys. Rev. D **106**, 035034 (2022).
[137] Yang Hwan Ahn, Sin Kyu Kang, and Raymundo Ramos, Implications of new CDF-II W boson mass on two Higgs doublet model, Phys. Rev. D **106**, 055038 (2022).
[138] Kodai Sakurai, Fuminobu Takahashi, and Wen Yin, Singlet extensions and W boson mass in light of the CDF II result, Phys. Lett. B **833**, 137324 (2022).
[139] Van Que Tran, Thong T. Q. Nguyen, and Tzu-Chiang Yuan, Obliquely scrutinizing a hidden SM-like gauge model, arXiv:2208.10971.
[140] Giorgio Arcadi and Abdelhak Djouadi, 2HD plus light pseudoscalar model for a combined explanation of the possible excesses in the CDF MW measurement and (g-2)μ with dark matter, Phys. Rev. D **106**, 095008 (2022).
[141] Karim Ghorbani and Parsa Ghorbani, W-boson mass anomaly from scale invariant 2HDM, Nucl. Phys. **B984**, 115980 (2022).
[142] H. Abouabid, A. Arhrib, R. Benbrik, M. Krab, and M. Ouchemhou, Is the new CDF M_W measurement consistent with the two Higgs doublet model? Nucl. Phys. **B989**, 116143 (2023).
[143] Francisco J. Botella, Fernando Cornet-Gomez, Carlos Miró, and Miguel Nebot, Muon and electron $g-2$ anomalies in a flavor conserving 2HDM with an oblique view on the CDF M_W value, Eur. Phys. J. C **82**, 915 (2022).
[144] Jinheung Kim, Soojin Lee, Prasenjit Sanyal, and Jeonghyeon Song, CDF W-boson mass and muon $g-2$ in a type-X two-Higgs-doublet model with a Higgs-phobic light pseudoscalar, Phys. Rev. D **106**, 035002 (2022).
[145] Stefan Hessenberger, Stephan Hessenberger, and Wolfgang Hollik, Two-loop improved predictions for M_W and $\sin^2\theta_{eff}$ in Two-Higgs-Doublet models, Eur. Phys. J. C **82**, 970 (2022).
[146] Tomohiro Abe, Ryosuke Sato, and Kei Yagyu, Lepton-specific two Higgs doublet model as a solution of muon $g-2$ anomaly, J. High Energy Phys. 07 (2015) 064.
[147] Yoshihiko Abe, Takashi Toma, and Koji Tsumura, A μ-τ-philic scalar doublet under Z_n flavor symmetry, J. High Energy Phys. 06 (2019) 142.
[148] David M. Straub, flavio: A Python package for flavour and precision phenomenology in the Standard Model and beyond, arXiv:1810.08132.
[149] F. James and M. Roos, MINUIT: A system for function minimization and analysis of the parameter errors and correlations, Comput. Phys. Commun. **10**, 343 (1975).
[150] Hans Dembinski, Piti Ongmongkolkul *et al.*, scikit-hep/iminuit, 10.5281/zenodo.3949207 (2020).
[151] D. Binosi and L. Theussl, JaxoDraw: A graphical user interface for drawing Feynman diagrams, Comput. Phys. Commun. **161**, 76 (2004).
[152] J. D. Hunter, Matplotlib: A 2d graphics environment, Comput. Sci. Eng. **9**, 90 (2007).
[153] Howard Georgi and Dimitri V. Nanopoulos, Suppression of flavor changing effects from neutral spinless meson exchange in gauge theories, Phys. Lett. **82B**, 95 (1979).
[154] L. Lavoura and Joao P. Silva, Fundamental CP violating quantities in a $SU(2) \times U(1)$ model with many Higgs doublets, Phys. Rev. D **50**, 4619 (1994).
[155] F. J. Botella and Joao P. Silva, Jarlskog-like invariants for theories with scalars and fermions, Phys. Rev. D **51**, 3870 (1995).